UDK 620.1:539.4.016:621.785:669.715
Original scientific article/Izvirni znanstveni članek

ISSN 1580-2949
MTAEC9, 55(2)283(2021)

INFLUENCE OF A LOW-TEMPERATURE PLASTIC-DEFORMATION PROCESS ON THE MICROSTRUCTURE OF AN Al-Si-Mg ALUMINUM ALLOY

VPLIV NIZKOTEMPERATURNE PLASTIČNE DEFORMACIJE NA MIKROSTRUKTURO ALUMINIJEVE ZLITINE Al-Si-Mg

Ceren Gode*

School of Denizli Vocational Technology, Program of Machine, Pamukkale University, Denizli, Turkey

Prejem rokopisa – received: 2020-09-22; sprejem za objavo – accepted for publication: 2020-12-29

doi:10.17222/mit.2020.187

This work was planned to modify the microstructure of a solution-treated, cast Al-Si-Mg aluminum alloy by a plastic deformation method at a cryogenic temperature. It was found that cryo-rolling is an efficient low-temperature, plastic-deformation method that causes the transformation of a dendritic microstructure to an ultrafine-grained counterpart with a high dislocation density and the redistribution of hard silicon particles in the cast aluminum alloy. The results show cryo-rolling strains lead to an increment of the dislocation density because of the annihilation of the dislocations' dynamic recovery. The microstructural refinement imposed by cryo-rolling seems to lead to a notable strength enhancement of the material because of the coupled impact of dislocation-strengthening and grain-boundary-strengthening mechanisms.

Keywords: Al-Si-Mg aluminum alloy, solution-treatment, cryo-rolling, microstructure, Williamson-Hall relationship, X-ray diffraction

V članku avtor opisuje modifikacijo mikrostrukture raztopno žarjene lite Al-Si-Mg zlitine s plastično deformacijo pri kriogenski temperaturi. Preizkušance je avtor pred valjanjem za 10 minut ohlajal v tekočem dušiku. V članku ugotavlja, da je kriogensko valjanje izbrane zlitine učinkovita metoda nizkotemperaturne plastične deformacije, s katero lahko povzročimo pretvorbo dendritne mikrostrukture v ultrafino zrnato mikrostrukturo z veliko gostoto dislokacij in prerazporeditvijo silicijevih delcev. Rezultati preizkusov so pokazali, da deformacije med kriovaljanjem povzročajo povečanje gostote dislokacij, ker je zavrta dinamična poprava dislokacij. Udrobljenje mikrostrukture, povzročeno s kriovaljanjem, tudi izboljša mehanske lastnosti zlitine zaradi istočasnih mehanizmov dislokacijskega utrjevanja in utrjevanja kristalnih mej.

Ključne besede: zlitina Al-Si-Mg, raztopno žarjenje, kriovaljanje, mikrostruktura, Williamson-Hallova enačba, rentgenska difrakcija

1 INTRODUCTION

From the past, aluminum and its alloys are one of the potential solutions for overcoming the concern of heavy materials. Nowadays, aluminum alloys are among the most utilized non-ferrous metals and alloys in advanced engineering applications. As is well known, aluminum in its purest form is too soft and ductile. Nevertheless, its strength can be improved remarkably by alloying. In this regard, aluminum can be alloyed with a wide variety of elements, each of them can induce special effects, hence leading to the formation of various grades of alloys with different benefits and application fields.[1–3]

Among them, an aluminum alloy including magnesium and silicon is a very common type of Al alloy owing to its novel behavior. It plays a powerful role in industrial operations in both cast and wrought conditions. One of these qualities is their unique formability, which allows them to be extruded into complex shapes applied to numerous structural purposes. Also, their mechanical properties can be improved by utilizing a proper heat-treatment operation due to their heat-treatability.[4] According to the lightweight feature coupled with good strength and ductility,[5,6] it can be employed in building the fuselage and wing structures of aircraft and due to its high-grade workability and great corrosion resistance, they can also be utilized for marine structures, both offshore and onshore.[7] Also, recent developments show its usage in bicycle frames and other components.

It should be noted that both wrought and cast forms of Al-Si-Mg alloys are utilized in wide application fields. As is well known, the cast form of this alloy is designed by 3xx.x, and the alloying content of silicon dominates over magnesium because the addition of silicon improves the fluidity of the alloy in the molten state, which inhibits premature solidification and therewith increases the castability of the material. However, the weak mechanical properties of the cast Al-Si-Mg alloy limit its application, consequently, for the extension of its application, it is essential to overcome the defects of this alloy.[3]

On the other hand, the mechanical properties of polycrystalline materials are considerably affected by their microstructure. Hence, the microstructure of the material can be adjusted in order to improve the mechan-

*Corresponding author's e-mail:
cgode@pau.edu.tr (Ceren Gode)

ical properties. Microstructural modification is made by subjecting the material to thermo-mechanical processing. It means that a synergetic impact of thermal energy along with the plastic deformation can be used to adjust the microstructure of the material. The modified microstructure enhances the mechanical performance of the alloy,[8] so a proper processing scheme should be chosen based on the industrial requirements.

The potential of an ultrafine-grained (UFG) microstructure to improve mechanical properties is widely investigated by numerous researchers.[9–11] It is mentioned that the material with the UFG microstructure has excellent mechanical performance as compared to their coarse-grained (CG) counterparts. This means the need for improvement of the available thermo-mechanical processing methods and the selection of proper processes. Therefore, they attempted to transform the existing microstructure to the UFG one, resulting in an optimum material with the minimum expenditure of energy during processing. The thermo-mechanical processing includes a low-temperature plastic deformation method that refines the microstructure of the material, leading to the formation of UFGs with the least imposed plastic strains.

Previous studies showed that the application of low-temperature plastic-deformation methods has two advantages over high-temperature counterparts. First, they can suppress dislocation annihilation by dynamic recovery, thus high strength can be attained with a low magnitude of plastic strain. Second, they stop dynamic precipitation, so the mechanical properties can be better by post-process aging operations. In this regard, cryo-rolling can be used as a possible low-temperature plastic-deformation method for effective microstructural refinement.[12–14] Wang et al. in 2002 cryo-rolled a pure Cu sample up to the intense plastic strain for attaining nanostructured material with better mechanical properties.[15] Although most works have been performed on the cryo-rolling of various metals and alloys, the studies on cast aluminum alloys are quite poor. In 2011, Markushev et al.[16] applied cryo-rolling to an Al-4.4% Cu cast alloy. However, a preprocess of equal channel angular pressing was performed before cryo-rolling to eliminate the cast dendritic microstructure. Few works[12,17–19] are also available in the literature about the cryo-rolling of in-situ Al composites that are manufactured with the stir-casting method. Nevertheless, a complete investigation of the microstructural evolution during cryo-rolling and the role of cryo-rolling strain on the particle refinement and microstructural modification of the aluminum matrix is still lacking. Hence, our work has been carried out with this goal.

As mentioned above, cast Al-Si-Mg alloys are potential materials for lightweight applications that require to be investigated further to increase their application. Imposing a large magnitude of plastic strains to form the UFG microstructure improves the mechanical properties of this alloy. Nevertheless, the plastic deformation applied until now consumed a great deal of energy to impose adequate grain refinement in these materials. Hence, there is an emerging requirement for performing a low-temperature plastic deformation method to refine the microstructure of a cast Al-Si-Mg alloy with lower energy. In this regard, cryo-rolling can be a proper method that imposes a considerable magnitude of plastic strains into the material with the least consumed energy. Also, the microstructure of this casting alloy is determined to be complex due to the dendritic matrix and a large number of silicon particles that are heterogeneously distributed in the aluminum matrix. This changes the overall microstructural development during cryo-rolling and also the mechanical performance of the cryo-rolled material.

2 MATERIALS AND METHOD

For this study, an Al-Si-Mg casting alloy was chosen. The chemical composition of the aluminum alloy obtained with optical emissive spectroscopy is 6.93 % Si, 0.55 % Mg, 0.17 % Mn, 0.16 % Cu, 0.12 % Fe, 0.09 % Ti, and aluminum as a base metal (in weight percent). According to the ASTM E1251 standard, it is an A357 aluminum alloy. First, the surface of the cast ingot was milled down to get rectangular blocks, and plates of 10 mm were sliced out from the rectangular blocks. The sliced plates were then finished to 8-mm thickness and the samples were cut to final dimensions of 8 mm × 30 mm × 50 mm. Afterwards, the sliced plates are subjected to a solution treatment at 540 °C for 8 h in a muffle furnace, followed by rapid cooling in cold water. Ultimately, the heat-treated sample is subjected to cryo-rolling. Cryo-rolling involves soaking the heat-treated plates in liquid nitrogen for 10 minutes and then they were rolled in a 100-mm-diameter rolling mill at a rate of 6 min^{-1}. Also, the ultimate thickness of 1 mm was obtained during the multiple passes, including a 0.2-mm reduction per pass. Overall, 35 pass numbers of the cryo-rolling process were carried out for this aim. Between every pass, the plates were immersed inside the liquid nitrogen for 10 minutes to maintain the uniformity of the processing temperature. It should be mentioned that although the amount of imposed plastic strain on the sample per each pass is nearly low, a higher amount of that per pass can cause a crack at the surface of the fabricated sheet because of the utilized low temperature of this process (–185 °C).

The microstructure of different aluminum conditions (as-cast, solution-treated, and solution-treated and cryo-rolled samples) was characterized using optical (OM), scanning electron (SEM), and transmission electron (TEM) microscopies. Phase identification of the materials was performed by X-ray diffraction (XRD). Also, XRD was applied to estimate the imposed microstrain and dislocation density existing in the samples. All the

samples were extracted from the cross-section that is perpendicular to the rolling direction and ground using SiC abrasive papers up to P3000 grit size. The sample was further polished to a mirror-like quality using diamond suspension down to 0.8 µm. The last polishing was performed with a colloidal silica of 0.2 µm. Keller's reagent (1 % HF, 1.5 % HCl, 2.5 % HNO_3, H_2O) was utilized to determine the constituents of the alloys. OM micrographs were taken with a Quasmo MR 5000 microscope. For this aim, the related standard metallographic process was done under the ASTM E3. The SEM images were performed using a Zeiss microscope operated at an accelerating voltage of 30 kV. In addition, TEM observations were conducted with a FEI Tecnai machine operating with a 200-kV accelerating voltage. In this regard, the specimens were mechanically reduced to 70-µm thickness and discs of 3 mm diameter were punched out from the thinned sheets. Final polishing was accomplished by a twin-jet electro-polishing machine with an electrolyte containing 20 % nitric acid and 80 % methanol at –30 °C. XRD was done using a Bruker AXS D8 Discover diffractometer with a copper source, K_α radiation (λ = 0,15 nm).

3 RESULTS AND DISCUSSION

Figure 1 displays the micrographs of the initial sample in the as-cast condition (AC). As can be observed, the AC sample contains large primary Al dendrites with needle-shaped Si particles (**Figure 1b**) segregated at the dendritic boundary (**Figure 1a**). In order to assess the composition of various elements in the phases shown in **Figure 1**, selective EDS analyses are performed on the phases of interest.

Table 1 lists the EDS analyses of the silicon particles (**Figure 1b**). The EDS result reveals that the silicon particles include both aluminum and silicon in equal proportions. Next to the Si particles and α-matrix, different phases can form due to some other alloying elements. It is found that the microstructure includes a high fraction of iron-based intermetallic particles. Accordingly, the manganese in the material combines with iron leading to the formation of the Fe-Mn intermetallic phase, as shown in **Figure 1c**. **Table 1** also shows the chemical composition of the particle Fe-Mn-rich intermetallic particle (**Figure 1c**). As is clear in **Figure 1d**, the interplay of Mg with Fe makes needle-shaped Mg-rich Fe-intermetallics. For the main precipitation strengthening the Mg_2Si phase is distributed in the eutectic region with a coarse Chinese-script structure (**Figure 1e**). The stoichiometric ratio of the Mg_2Si phase according to the EDS analysis is listed in **Table 1**. The AC sample is then subjected to heat treatment (solution heat treatment) before processing the material using the cryo-rolling method.

Table 1: EDS analyses of silicon particle (shown in **Figure 1b**), Fe-Mn based intermetallic (shown in **Figure 1c**), and Mg_2Si phase (shown in **Figure 1e**)

	Related to **Figure 1b**	Related to **Figure 1c**	Related to **Figure 1e**
Element	Weight percent / Atomic percent		
Mg	0.45/0.51	0.76/0.92	7.36/8.24
Al	43.35/44.52	60.39/66.18	85.09/85.85
Si	55.26/54.51	23.55/24.80	4.74/4.60
Mn	0.34/0.17	5.52/2.97	0.62/0.31
Fe	0.35/0.17	8.94/4.73	1.11/0.54
Cu	0.26/0.11	0.85/0.39	1.08/0.46

It is shown that the AC sample has a dendritic microstructure with needle-shaped sharp Al-Si eutectic particles filling the inter-dendritic region. After the solution treatment (ST) procedure, the aspect ratio of the needle-shaped particles has decreased and transformed into a spherical/elliptical shape. A higher-magnification optical microscopic image shows the comparison of particle morphology between the AC and ST samples (**Figure 2**).

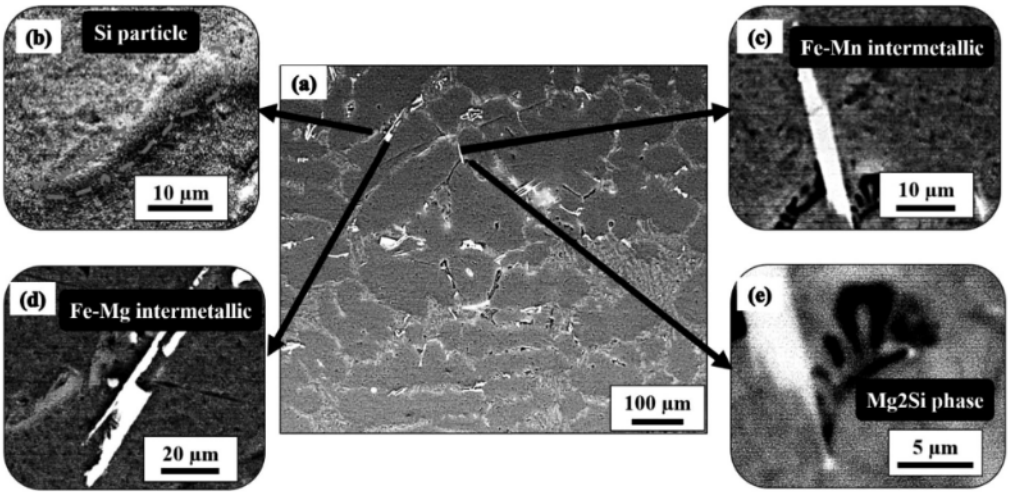

Figure 1: SEM micrograph of as-cast sample: a) dendritic microstructure, b) needled-shaped Si particle, c) and d) Fe-Mn and Fe-Mg intermetallic compounds in sequence, and e) Mg_2Si intermetallic compound recognized as the dark script-like structure

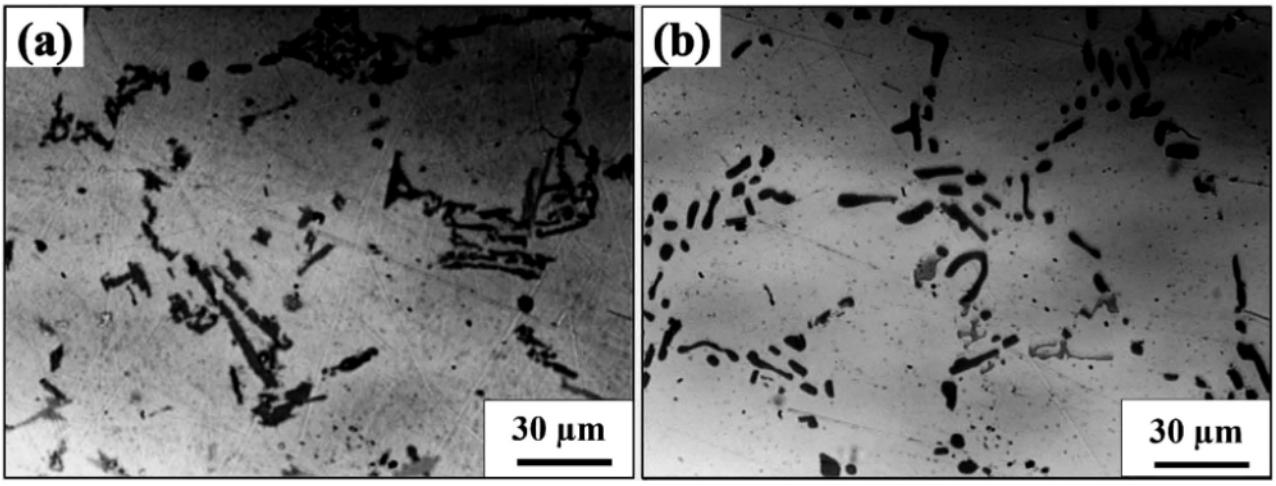

Figure 2: Optical micrographs of: a) as-cast and b) solution-treated samples representing the silicon particles morphology

According to **Figure 2**, two notable changes happen in the material microstructure through solution treatment. The silicon particles have begun to spheroidize slightly and the aluminum matrix has been partly homogenized and has become supersaturated in alloying elements. As the AC sample is applied by the solution-treatment operation, different microstructure differences occur that are illustrated with the aid of a typical phase diagram of the Al-Si alloy. Accordingly, the solid-solubility of Si in Al in the ambient temperature is just 0.05 *w*/% and any composition exceeding this leads to a second-phase forming. On the other hand, the high-temperature solubility of Si at 540 °C is nearly 1.2 *w*/%.[20–22]

The studying material includes about 6.93 *w*/% of Si and consequently at elevated temperature, a portion of the Al-Si eutectics dissolves into the α-aluminum matrix. Because of the great surface energy for the sharp edges of the aforementioned eutectic particles, the atoms in those zones diffuse into the aluminum matrix. This dissolution transforms the shape of the Si particles to a near-sphere shape, so the procedure of solution treatment is referred to as the spheroidization treatment in the literature.[23–25] It should be mentioned that magnesium also has a great solubility gradient with temperature. The weight percentage of magnesium in the present material is 0.55. Because of the lower amount of Mg, as compared to its maximum solubility range in aluminum, the Mg_2Si phase is anticipated to be entirely dissolved in the α-aluminum matrix upon solution treatment at 540 °C. It is clear that in the room temperature state, the amount of silicon and other alloying atoms that can be held in the aluminum lattice is less. Nevertheless, the rapid cooling process does not permit the entrapped alloying atoms to diffuse out of the aluminum matrix. This causes a condition where the matrix becomes supersaturated with solute atoms and consequently, the final solution-treated situation of the material is a supersaturated solid solution. It should be noted that the effect of post-solutionized precipitation treatment will be studied in the next work.

In the following, the role of the cryo-rolling process on the microstructural refinement of the aluminum sample is discussed and divided into two sections for a better assessment. One is the effect of rolling plastic strain on the silicon particles and the other is the effect of rolling plastic strain on the aluminum matrix. **Figure 3** shows three-dimensional microstructural views on the overall distribution of silicon particles in the material and its development with the cryo-rolling plastic strain for the as-cast, solution-treated, and cryo-rolled specimens (SCR-50 and SCR). It should be noted that the SCR-50 is an intermediate material condition where cryo-rolling is up to 50 % of thickness reduction to explain the development of microstructure during cryo-rolling.

The particle distribution in the AC sample is dendritic. Also, their dendritic distribution is found to be isotropic with similar dendritic arm spacing in all direc-

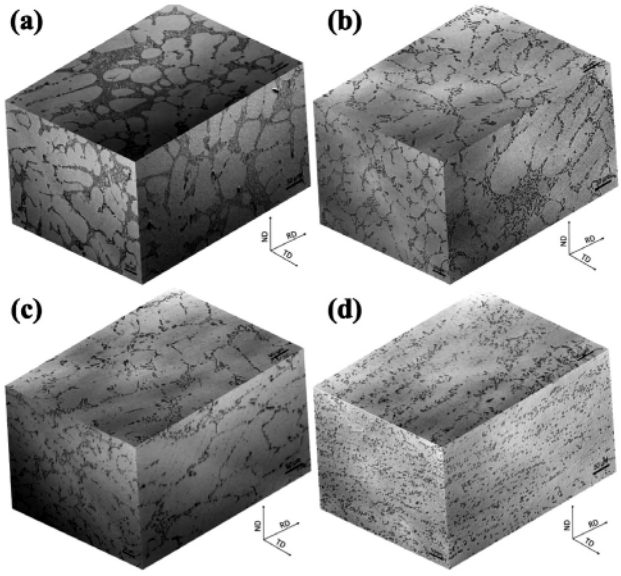

Figure 3: Microstructure images of: a) as-cast, b) solution-treated, c) solution-cryo-rolled with 50 % thickness reduction, and d) solution-cryo-rolled samples (the scale bar is 50 µm)

tions according to **Figure 3a**. The distribution is changed after solution treatment; nevertheless, the morphology of silicon particles is altered in the ST sample because of spheroidization (**Figure 3b**). No meaningful particle redistribution is recognized in the SCR-50 sample. However, the rolling strain displaces plastically the aluminum matrix for the rolling and normal axes (direction) because of the shear and compressive conditions, respectively. Consequently, the dendritic structure of the AC and ST samples is converted to the elongated-dendritic microstructure through the lower cryo-rolling plastic strain (SCR-50) (**Figure 3c**). By the increment of plastic strains, the particles become more homogenized in the aluminum matrix, as can be seen in the SCR sample (**Figure 3d**). Since the large thickness reduction induces more extra compressive plastic strains into the sample in the normal direction, the particle distribution is found to be more uniform in the RD and TD planes in comparison with that in the ND plane.

The quantitative data on the particle morphological aspects including the size and aspect ratio are measured from the optical micrographs based on the image-processing technique using ImageJ. In this regard, the size of the particle was measured by the relationship of P/π in which P is the perimeter of the Si particle. Nearly 400 particles per sample position were used to draw the histograms. The smallest particle size was considered to be 1 μm. For determining the aspect ratio, they were considered to be a complete ellipse and the aspect ratio is determined as the ratio within the major and minor axes. **Figures 4** and **5** show the size and aspect ratio of Si particles for the as-cast, solution-treated, solution-cryo-rolled with a 50 % thickness reduction, and solution-cryo-rolled samples, respectively.

The size and aspect ratio of Si particles for the initial sample is found to be distributed in the range 1–18 μm (**Figure 4a**) and 1–8 μm (**Figure 4e**), respectively. After the solution-treated operation, the size distribution trend converges towards the lowest particle sizes (**Figure 4b**). Also, the shape of the particles approaches that of a sphere as their aspect ratio decreases (**Figure 4f**). The diffusion of secondary elements from the sharp edges into the matrix could be the reason for the decrease in the size and aspect ratio of the particles for the ST sample. At the intermediate stage of the cryo-rolling (SCR-50), the size of the particles is found to be less than that of ST material (**Figure 4c**). However, the aspect ratio of these particles is found to be larger than that of both ST and SCR samples (**Figure 4g**). In the final cryo-rolled material (SCR), 43 % of the particles are smaller than 3 μm and nearly 49 % of the Si particles is in the order of 1–4 μm (**Figure 4d**). More than ¾ of the particles (79 %) have an aspect ratio of less than 2 μm in the SCR sample (**Figure 4h**), similar to that of the ST sample.

Figure 5 shows the refinement of silicon particles through the cryo-rolling from the base ST condition.

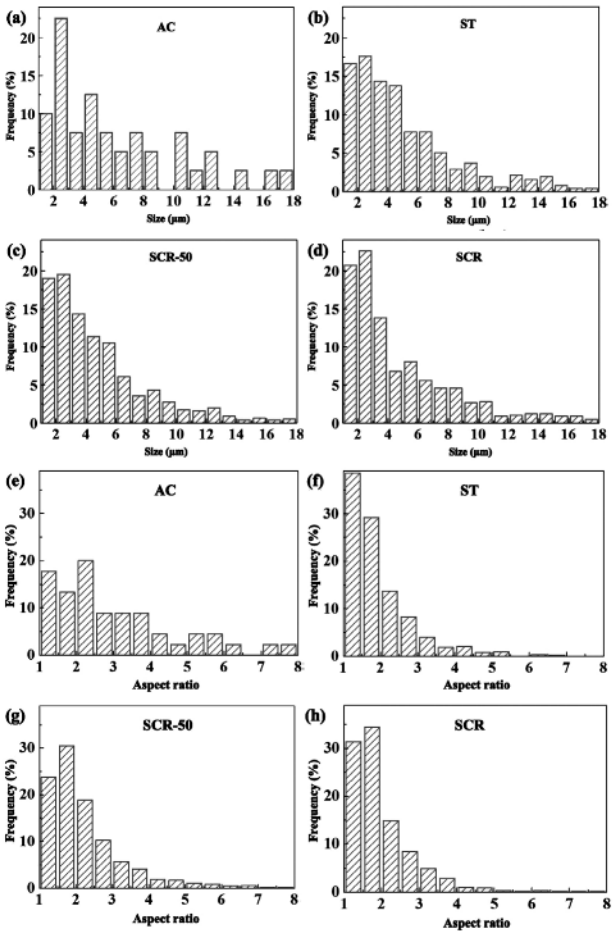

Figure 4: Plots of the silicon particle size and aspect ratio in a and e) as-cast b and f) solution-treated c and g) solution-cryo-rolled with 50 % thickness reduction, and d and h) solution-cryo-rolled samples

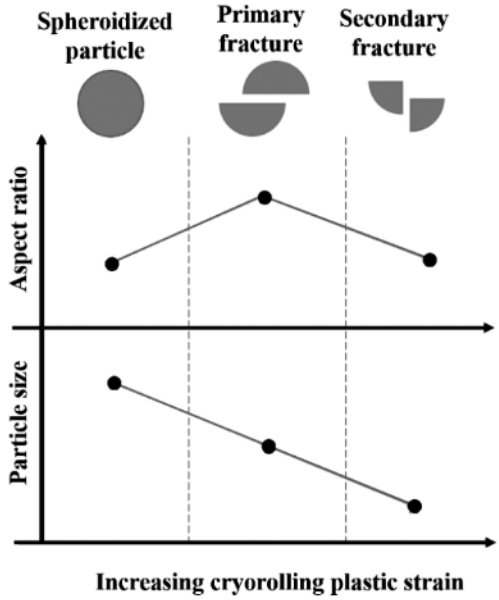

Figure 5: Schematic representation displaying the effect of cryo-rolling on the size and aspect ratio of silicon particle in A357 aluminum alloy

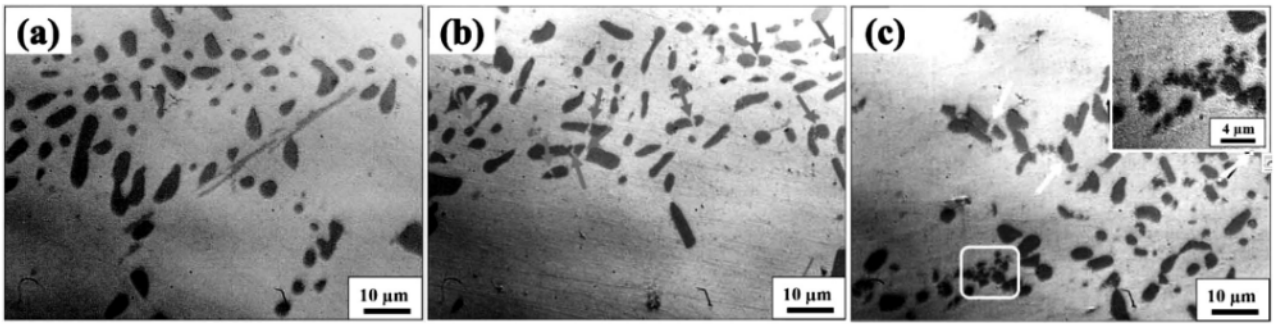

Figure 6: Optical microscopy images of: a) solution-treated, b) solution-cryo-rolled with 50 % thickness reduction, and c) solution-cryo-rolled samples displaying the silicon particle morphology before and after cryo-rolling

During the primary step of the cryo-rolling (SCR-50), the Si particle with a great aspect ratio breaks down at first shown with arrows in **Figure 6b**. By rolling up to 87.5 % plastic strain (SCR), the fractured particles become refined more by means of secondary fracture (**Figure 6c**). The results indicate that the primary aspect ratio of the Si particles is less because of the spheroidization (**Figure 4b**) and it rises by the decrease in size if they shear through cryo-rolling. Moreover, the sheared particles have been subjected to more shear by the addition of the plastic strain (secondary shear). This event reduces the size and aspect ratio of the Si particles (**Figure 6**).

The microstructural development in the A357 aluminum alloy during cryo-rolling is examined by TEM and XRD. The TEM images of SCR-50 and SCR samples are shown in **Figure 7**. The aforementioned plastic deformation process at cryogenic temperature produces a high density of dislocations in the aluminum matrix. Because this process happens at low temperature, dynamic recovery of the dislocations is restrained; therefore, the dislocation density keeps on increasing by cryo-rolling plastic strains. As the matrix is overfilled by the dislocations, they lead to make cell substructures (polygonization).[26] The appearance of such sub-cell structures is seen in the TEM image of the SCR-50 sample (**Figure 7a**). As the

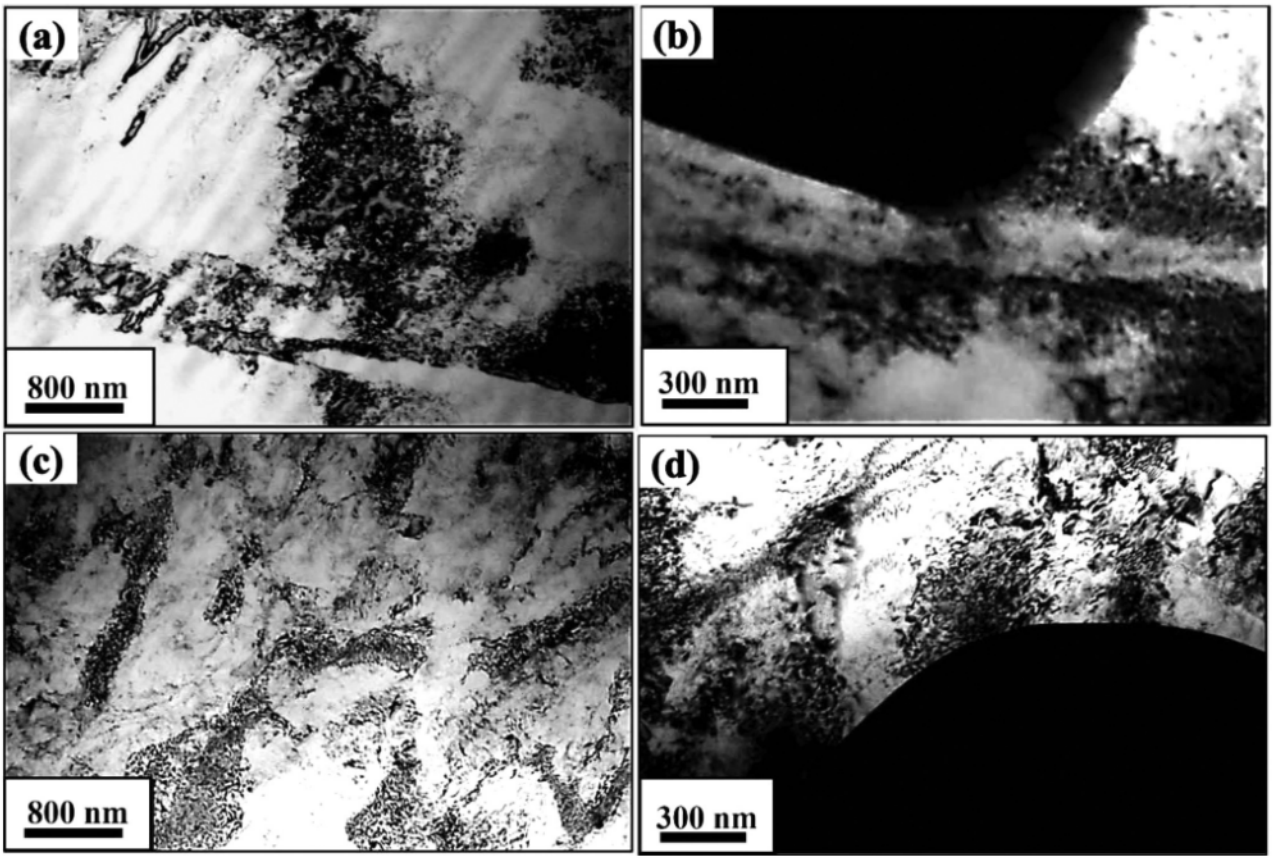

Figure 7: Transmission electron microscopy of: a) and b) solution-cryo-rolled with 50 % thickness reduction and c) and d) solution-cryo-rolled samples

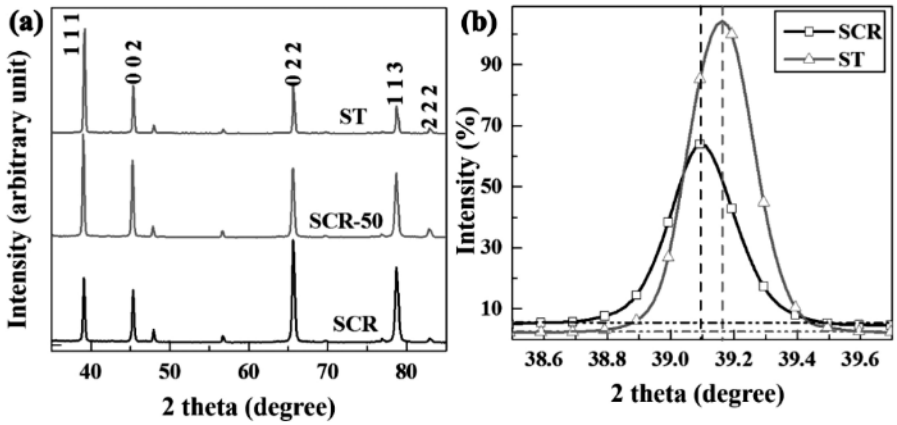

Figure 8: a) XRD patterns of solution-treated, solution-cryo-rolled with 50 % thickness reduction, and solution-cryo-rolled samples and b) the magnified view of the [111] peak of aluminum in both the ST and SCR conditions

cryo-rolling plastic strains increase, the sub-grain structures become refined, leading to a finer grain structure in the SCR sample (**Figure 7c**). At the particle-matrix interfacial region, the Si particles prevent the movement of the dislocations; therefore, the dislocations have been pinned. This causes more dislocation accumulation within the interface. Ultimately, the grain structure is found to be finer in the interface zone (**Figure 7b** and **7d**) than in the central region of the aluminum matrix.

As mentioned above, the X-ray diffraction method is employed to quantify the imposed magnitude of microstrain and dislocations density in different material conditions. [27] The XRD patterns of ST, SCR-50, and SCR samples are presented in **Figure 8**. Indeed, **Figure 8a** is related to the XRD pattern of ST, SCR-50 and SCR samples, and **Figure 8b** shows the enlarged image of the [111] peak of the aluminum at the ST and SCR conditions. Also, the vertical and horizontal lines in **Figure 8b** exhibit the peak centers and background intensities in sequence. The results show that the peak height pattern alters from ST to SCR, which is due to the texture induced because of the rolling plastic strains. A magnified image of the [111] peak of aluminum at the ST and SCR conditions confirms that the [111] peak has moved to the smaller 2θ angles after cryo-rolling, which is associated with the intense compressive plastic strains due to the cryo-rolling process.

The accumulation of dislocations is calculated according to the broadening of XRD peaks. Dislocations density (ρ) of the materials are obtained using the equation of Equation (1)[28] in which b is the Burgers vector, d is the crystallite size and ε is the root mean square of the microstrain taken at different crystallographic axes. It should be mentioned that both the crystallite size and the microstrain are determined by the Williamson-Hall method.[29] This method utilizes the broadening of a peak arising from the crystallite size and the strain that is provided with the Equation (2). In this relationship, B is full width at half maximum (FWHM), θ is the Bragg angle, K is a constant, and λ is the wavelength of the incident radiation.[30] Furthermore, for obtaining the crystallite size and microstrain, the peak width of the instrumental broadening should be compensated. Accordingly, the XRD pattern of an annealed material has been attained. The calculated dislocation density and the imposed microstrain magnitude are listed in **Table 2**.

$$\rho = \frac{2\sqrt{3}\varepsilon}{\mathrm{d}b} \tag{1}$$

$$B\cos\theta = \frac{K\lambda}{d} + \varepsilon\sin\theta \tag{2}$$

Table 2: Dislocations density of a solution-treated, solution-cryo-rolled with 50 % thickness reduction, and solution-cryo-rolled samples

Sample condition	Crystallite size (A)	Microstrain (%)	Dislocations density (10^{14} m^{-2})
ST	31813.1	0.052	1.99
SCR-50	1634.75	0.122	90.24
SCR	898.67	0.101	136.67

It is found that a sharp increase in dislocation density is observed in the sample after cryo-rolling along with the decrease in the crystallite size. Also, the microstrain in the sample displays an increasing trend from the ST to the SCR-50 condition, and then it decreases for the SCR situation. This is due to the grain refinement with increasing cryo-rolling passes. As the substructure results with the grain refinement, the lattice dislocation reduces by the increment of the cell boundary dislocations. The aforementioned causes an increment in the density of boundaries. Moreover, the boundaries that limit the cell structures retain their non-preferred orientations. [31,32]

4 CONCLUSIONS

The present work investigated the microstructural development of a cast Al-Si-Mg aluminum alloy through one of the well-known thermo-mechanical processing

termed cryo-rolling. The main conclusions are as follows:

- The large primary aluminum dendrites with needle-shaped Si particles segregated in the dendritic boundaries of the as-cast sample are transformed into the spheroidization of Si particles and homogenization/supersaturation of the aluminum matrix through the solution-treatment. It should be mentioned that the distribution of the particles is changed after the solution-treatment and their morphology is also altered due to the spheroidization.
- It was shown that the sub-grain structures become more refined, leading to a finer grain structure in the final sample by increasing the magnitude of the cryo-rolling plastic strains. Additionally, the XRD indicated that a sharp increase in the dislocation density of the final sample is accompanied by a decrease in the crystallite size.
- After cryo-rolling, the aspect ratio of more than ¾ of the particles is less than 2 μm, which is almost equal to that of the solution-treated sample.
- The achieved results indicated that cryo-rolling is an effective low-temperature plastic deformation method in which notable grain refinement is obtained in the sample with the least magnitude of imposed plastic strain.

5 REFERENCES

[1] M. Kamp, J. Bartsch, R. Keding, M. Jahn, R. Müller, M. Glatthaar, S.W. Glunz, I. Krossing, Plating processes on aluminum and application to novel solar cell concepts, Energy Procedia. 55 (**2014**) 679–687, doi:10.1016/j.egypro.2014.08.044

[2] E. A. Starke, J. T. Staleyt, Application of modern aluminum alloy to aircraft, Prog. Aerosp. Sci. 32 (**1996**) 131–172, doi:10.1016/0376-0421(95)00004-6

[3] J. A. Taylor, D. H. Stjohn, M. A. Easton, Case studies in aluminium casting alloys, Woodhead Publishing Limited, **2010**, doi:10.1533/9780857090256.1.185

[4] P. Nageswara rao, R. Jayaganthan, Effects of warm rolling and ageing after cryogenic rolling on mechanical properties and microstructure of Al 6061 alloy, Mater. Des. 39 (**2012**) 226–233, doi:10.1016/j.matdes.2012.02.010

[5] F. Rajabi, A. Zarei-Hanzaki, M. Eskandari, S. Khoddam, The effects of rolling parameters on the mechanical behavior of 6061 aluminum alloy, Mater. Sci. Eng. A., 578 (**2013**) 90–95, doi:10.1016/j.msea.2013.04.023

[6] S. Das, N. S. Lim, H. W. Kim, C. G. Park, Effect of rolling speed on microstructure and age-hardening behaviour of Al-Mg-Si alloy produced by twin roll casting process, Mater. Des., 32 (**2011**) 4603–4607, doi:10.1016/j.matdes.2011.03.057

[7] N. Saleema, D. K. Sarkar, R. W. Paynter, D. Gallant, M. Eskandarian, A simple surface treatment and characterization of AA 6061 aluminum alloy surface for adhesive bonding applications, Appl. Surf. Sci., 261 (**2012**) 742–748, doi:10.1016/j.apsusc.2012. 08.091

[8] R. Z. Valiev, T. G. Langdon, Principles of equal-channel angular pressing as a processing tool for grain refinement, Prog. Mater. Sci., 51 (**2006**) 881–981, doi:10.1016/j.pmatsci.2006.02.003

[9] M. Ebrahimi, S. Attarilar, C. Gode, F. Djavanroodi, Damage prediction of 7025 aluminum alloy during equal-channel angular pressing, Int. J. Miner. Metall. Mater., 21 (**2014**) 990–998, doi:10.1007/s12613-014-1000-z

[10] M. Ebrahimi, H. Gholipour, F. Djavanroodi, A study on the capability of equal channel forward extrusion process, Mater. Sci. Eng. A., 650 (**2015**) 1–7, doi:10.1016/j.msea.2015.10.014

[11] C. Xu, S. Schroeder, P. B. Berbon, T. G. Langdon, Principles of ECAP-Conform as a continuous process for achieving grain refinement: Application to an aluminum alloy, Acta Mater., 58 (**2010**) 1379–1386, doi:10.1016/j.actamat.2009.10.044

[12] N. N. Krishna, K. Sivaprasad, P. Susila, Strengthening contributions in ultra-high strength cryorolled Al-4%Cu-3%TiB2 in situ composite, Trans. Nonferrous Met. Soc. China (English Ed.), 24 (**2014**) 641–647, doi:10.1016/S1003-6326(14)63106-X

[13] G. Purcek, H. Yanar, O. Saray, I. Karaman, H. J. Maier, Effect of precipitation on mechanical and wear properties of ultrafine-grained Cu–Cr–Zr alloy, Wear., 311 (**2014**) 149–158, doi:10.1016/j.wear.2014.01.007

[14] S. K. Panigrahi, R. Jayaganthan, A study on the mechanical properties of cryorolled Al-Mg-Si alloy, Mater. Sci. Eng. A., 480 (**2008**) 299–305, doi:10.1016/j.msea.2007.07.024

[15] W. Yinmin, C. Mingwei, Z. Fenghua, M. En, High tensile ductility in a nanostructured metal, Nature, 419 (**2002**) 912, doi:10.1038/nature01133

[16] M. V. Markushev, E. V. Avtokratova, I. Y. Kazakulov, S. V. Krymsky, M. Y. Mochalova, M. Y. Murashkin, O. S. Sitdikov, Microstructure and properties of an aluminum D16 alloy subjected to cryogenic rolling, Russ. Metall., 2011 (**2011**) 364–369, doi:10.1134/S0036029511040136

[17] N. M. Anas, B. K. Dhindaw, H. Zuhailawati, T. K. Abdullah, A. S. Anasyida, Effect of Initial Microstructure on Properties of Cryorolled Al 5052 Alloy Subjected to Different Annealing Treatment Temperatures, J. Mater. Eng. Perform., 27 (**2018**) 6206–6217, doi:10.1007/s11665-018-3645-7

[18] S. V. Zherebtsov, G. S. Dyakonov, A. A. Salem, V. I. Sokolenko, G. A. Salishchev, S. L. Semiatin, Formation of nanostructures in commercial-purity titanium via cryorolling, Acta Mater., 61 (**2013**) 1167–1178, doi:10.1016/j.actamat.2012.10.026

[19] T. Konkova, S. Mironov, A. Korznikov, S. L. Semiatin, Microstructural response of pure copper to cryogenic rolling, Acta Mater., 58 (**2010**) 5262–5273, doi:10.1016/j.actamat.2010.05.056

[20] C. M. Cepeda-Jiménez, J. M. García-Infanta, A. P. Zhilyaev, O. A. Ruano, F. Carreño, Influence of the thermal treatment on the deformation-induced precipitation of a hypoeutectic Al-7 wt% Si casting alloy deformed by high-pressure torsion, J. Alloys Compd., 509 (**2011**) 636–643, doi:10.1016/j.jallcom.2010.09.122

[21] Z. Chen, Y. Lei, H. Zhang, Structure and properties of nanostructured A357 alloy produced by melt spinning compared with direct chill ingot, J. Alloys Compd., 509 (**2011**) 7473–7477, doi:10.1016/j.jallcom.2011.04.082

[22] G. Sha, H. Möller, W. E. Stumpf, J. H. Xia, G. Govender, S. P. Ringer, Solute nanostructures and their strengthening effects in Al-7Si-0.6Mg alloy F357, Acta Mater., 60 (**2012**) 692–701, doi:10.1016/j.actamat.2011.10.029

[23] E. Ogris, A. Wahlen, H. Lüchinger, P. J. Uggowitzer, On the silicon spheroidization in Al-Si alloys, J. Light Met., 2 (**2002**) 263–269, doi:10.1016/S1471-5317(03)00010-5

[24] E. Sjölander, S. Seifeddine, The heat treatment of Al-Si-Cu-Mg casting alloys, J. Mater. Process. Technol., 210 (**2010**) 1249–1259, doi:10.1016/j.jmatprotec.2010.03.020

[25] M. Zhu, Z. Jian, G. Yang, Y. Zhou, Effects of T6 heat treatment on the microstructure, tensile properties, and fracture behavior of the modified A356 alloys, Mater. Des., 36 (**2012**) 243–249, doi:10.1016/j.matdes.2011.11.018

[26] M. Moradi, M. Nili-Ahmadabadi, B. Poorganji, B. Heidarian, M. H. Parsa, T. Furuhara, Recrystallization behavior of ECAPed A356 alloy at semi-solid reheating temperature, Mater. Sci. Eng. A., 527 (**2010**) 4113–4121, doi:10.1016/j.msea.2010.03.021

[27] I. Feijoo, M. Cabeza, P. Merino, G. Pena, M. C. Pérez, S. Cruz, P. Rey, Estimation of crystallite size and lattice strain in nano-sized TiC

particle-reinforced 6005A aluminium alloy from X-ray diffraction line broadening, Powder Technol., 343 (**2019**) 19–28, doi:10.1016/j.powtec.2018.11.010

[28] A. Sajadi, M. Ebrahimi, F. Djavanroodi, Experimental and numerical investigation of Al properties fabricated by CGP process, Mater. Sci. Eng. A., 552 (**2012**) 97–103, doi:10.1016/j.msea.2012.04.121

[29] K. Ma, H. Wen, T. Hu, T. D. Topping, D. Isheim, D. N. Seidman, E. J. Lavernia, J. M. Schoenung, Mechanical behavior and strengthening mechanisms in ultrafine grain precipitation-strengthened aluminum alloy, Acta Mater., 62 (**2014**) 141–155, doi:10.1016/j.actamat.2013.09.042

[30] H. Wen, T. D. Topping, D. Isheim, D. N. Seidman, E. J. Lavernia, Strengthening mechanisms in a high-strength bulk nanostructured Cu-Zn-Al alloy processed via cryomilling and spark plasma sintering, Acta Mater., 61 (**2013**) 2769–2782, doi:10.1016/j.actamat.2012.09.036

[31] V. Yamakov, D. Wolf, S. R. Phillpot, H. Gleiter, Grain-boundary diffusion creep in nanocrystalline palladium by molecular-dynamics simulation, Acta Mater., 50 (**2002**) 61–73, doi:10.1016/S1359-6454(01)00329-9

[32] Z. T. Trautt, Y. Mishin, Grain boundary migration and grain rotation studied by molecular dynamics, Acta Mater., 60 (**2012**) 2407–2424, doi:10.1016/j.actamat.2012.01.008